

## ELECTROCHEMICAL SENSING OF H<sub>2</sub>O<sub>2</sub> BY HYDROTHERMALLY SYNTHESIZED PURE COPPER OXIDE MATERIALS

M. E. MAZHAR<sup>a</sup>, R. ASIF<sup>a</sup>, A. WAHEED<sup>b</sup>, J. AHMAD<sup>a</sup>, M. N. USMANI<sup>a,\*</sup>, I. SYED<sup>c</sup>, H. M. KHAN<sup>d</sup>, I. AHMAD<sup>a</sup>, R. NAZ<sup>e</sup>, S. AHMAD<sup>f</sup>, W. ABBAS<sup>a</sup>, M. MAHMOOD<sup>a</sup>

<sup>a</sup>Department of Physics, Bahauddin Zakariya University, Multan, Pakistan

<sup>b</sup>Department of Geotechnical Engineering, MCE (NUST), Risalpur, Pakistan

<sup>c</sup>Department of Computer Science, The Superior College Lahore, Pakistan

<sup>d</sup>Department of Physics, The Islamia University of Bahawalpur, Bahawalpur-63100, Pakistan

<sup>e</sup>School of Material Science and Engineering, Shanghai Jiao Tong University, Dongchuan Road, Shanghai, 200240, P. R. China

<sup>f</sup>Department of Building and Architectural Engineering, UCE&T, Bahauddin Zakariya University, Multan. Pakistan

We report the variations in structural and morphological properties of hydrothermally synthesized pure CuO materials, prepared by employing three different stoichiometric concentrations of reagents (details given in experimental section), followed by autoclaving at different temperatures e. g. 160°C and 180°C for 6 hours. X-ray diffraction (XRD) revealed the presence of single (monoclinic: CuO) and mixed (monoclinic as well as cubic Cu<sub>2</sub>O) phases of copper oxide and cupric oxide respectively. Scanning Electron Microscopy (SEM) images reveal irregular distribution of particles having non-uniform grain shapes of all prepared materials except for the one having pure monoclinic structure. Most of the materials had comparable morphologies whereby sharp edges and flat surfaces of particle were observed. The particle size was ranging between 2µm to 4µm. One of the samples (having pure monoclinic structure) was further characterized for dc-electrical conductivity followed by electrochemical detection of H<sub>2</sub>O<sub>2</sub>. Results show appreciable ability of the material towards H<sub>2</sub>O<sub>2</sub> detection for concentrations as low as 2mM.

(Received August 6, 2020; Accepted December 21, 2020)

**Keywords:** Hydrothermal synthesis, Copper oxide, Hydrogen peroxide detection, Electrochemical sensing of H<sub>2</sub>O<sub>2</sub>

### 1. Introduction

Researchers around the world have been studying Copper Oxide (CuO) materials from decades due to their fascinating properties and numerous applications in various fields. CuO is classified as a p-type semiconducting material exhibiting a narrow band gap [1]. Several synthesis procedures can be used to synthesize and control the morphology of metal oxide materials but we adopted hydrothermal method for the purpose due to its multiple advantages over the others, including but not limited to simplicity, phase purity and uniformity as well as better control over the synthesis conditions. CuO has extensive range of industrial applications such as solar cell [2], gas sensor [3], antimicrobials [4], lithium ion batteries [5], photo-catalyst [6], fuel cells [1] and super capacitor [7]. All the physical and chemical properties of copper oxide are dependent on its micro-structure and morphology. Recently, Copper oxide

---

\* Corresponding author: naumanusmani@bzu.edu.pk

nanostructures including nanoparticles, nanotubes, nanobelts, nanoflowers, nanosheets, nanorods, and nanoneedles have been synthesized using various methods [8]. Copper oxide nanomaterials have been synthesized by various methods such as precipitation method, decomposition method, plasma methods, pulsed wire explosion method, vapor deposition method [9], hydrothermal method [10], sol-gel method [11], electrochemical method [12], radiolysis method and green method [13]. Copper Oxide is a promising metal of active electrode material for electrochemical sensor. Recently, copper oxide non-enzymatic sensor for hydrogen peroxide detection has been synthesized [14, 15, 16].

Copper oxide nanorods are used in sensing application of hydrogen peroxide [17]. Zang et.al fabricated an electrochemical sensor based on copper oxide nanoflower [18].

In this study, we report the synthesis of CuO nanomaterials via hydrothermal method. The morphology was investigated by SEM and the electrochemical behavior of  $H_2O_2$  on CuO/GCE modified electrode was explored. The manufactured sensor exhibited high sensitivity, selectivity and long term stability.

## **2. Experimental details**

### **2.1. Chemicals and reagents**

Copper chloride ( $CuCl_2 \cdot 2H_2O$ ) and potassium hydroxide (KOH) were used as precursor and precipitating agents respectively. All these reagents were of analytical grade and used without further purification. Deionized distilled water was used all over the experiment.

### **2.2. Synthesis of Copper Oxide Nanomaterials**

Copper oxide nanomaterials were synthesized via hydrothermal method on two dissimilar temperatures ( $160^\circ C$  and  $180^\circ C$ ) using three schemes: A (30ml+30ml), B (40ml+20ml), and C (50ml+10ml). In a usual procedure, three separate solutions of 0.1M ( $CuCl_2 \cdot 2H_2O$ ) (170.48 g/mol) were dissolved in 120ml of distilled water under constant magnetic stirring. In 100ml distilled water three separate solutions of 0.1M potassium hydroxide KOH (132.6 g/mol) were prepared. The precipitating agent KOH was added in three separate solutions drop wise under continuous stirring. All the prepared solutions were transferred into three Teflon lined stainless autoclaves. The autoclaves were sealed, maintained at  $180^\circ C$  for 8h, and then cooled down at room temperature naturally. The obtained green precipitates were washed with ethanol and distilled water many times and then dried in oven at  $80^\circ C$  for 4h. All the dried samples were grinded in mortar pestle and annealed at  $450^\circ C$  for 4h.

## **3. Results and discussion**

### **3.1. Structural analysis**

The structural analysis of Copper Oxide was disclosed by X-ray diffraction (XRD). Figure 1 shows the XRD pattern of samples(1-6). The diffraction peaks of sample1 can be indexed as (110), (002), (111), (202), (020), (311), (220) and (113) planes of a monoclinic copper oxide JCPDS Card no (05-0661). The Nelson Relay technique was used to calculate accurate lattice constant ( $a = 5.42^\circ A$ ) and average particle size (14.9 nm). The XRD patterns of samples (2-6) show that all peaks are associated with JCPDS Card no (02-1040, 44-0706) and (05-0667) with monoclinic and cubic structure respectively. The red indexing indicates the formation of CuO and blue indexing indicates the formation of  $Cu_2O$ . Some unidentified peaks at angle  $24.5^\circ$ ,  $34.5^\circ$ ,  $54.5^\circ$ ,  $55.5^\circ$  and  $64.5^\circ$  were observed due to incomplete reaction. Only XRD spectrum of sample 1 exhibits peaks that are associated to the single phased (CuO) monoclinic structure. Rest of the materials exhibit mixed phase formation.

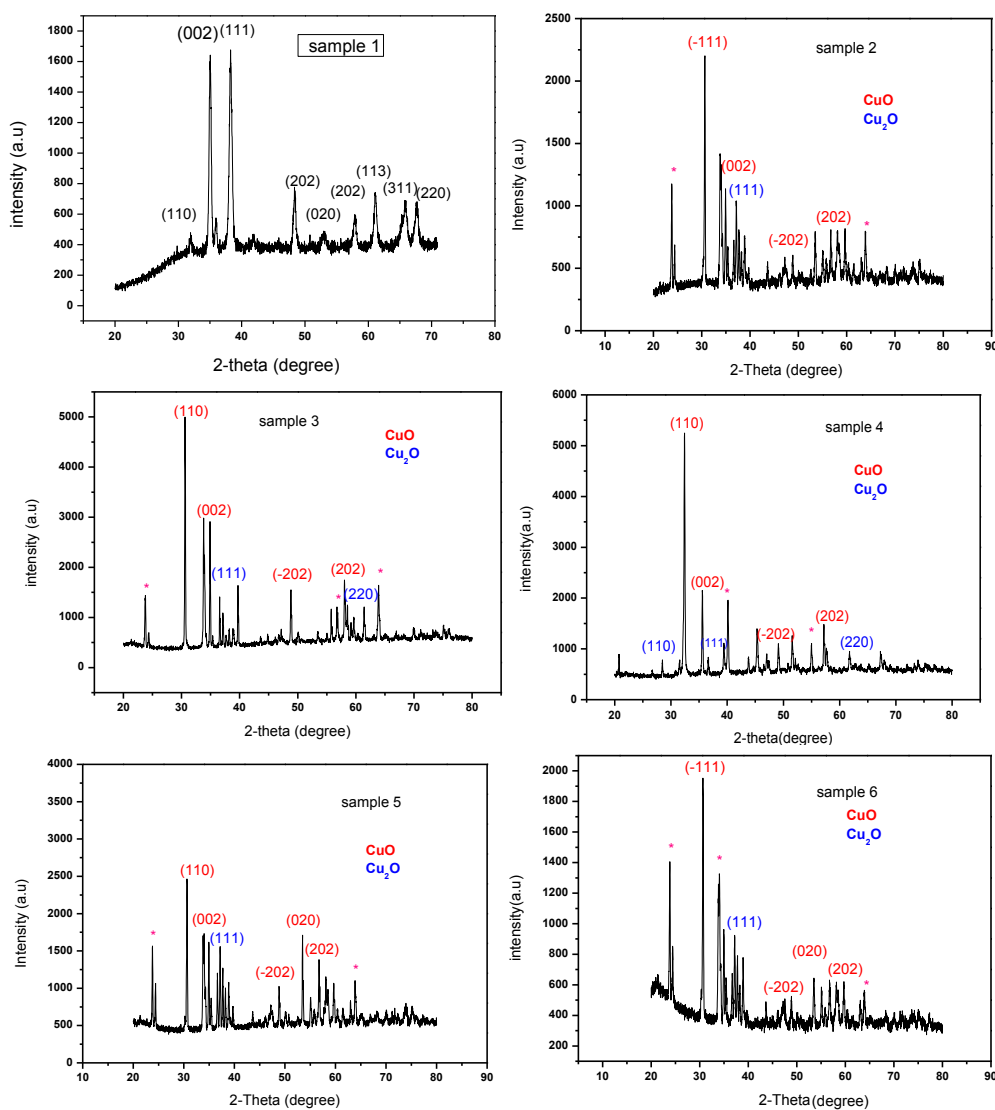


Fig. 1. X-ray diffraction (XRD) patterns of samples 1-6.

### 3.2. Morphological analysis

The morphological analysis of CuO nanomaterials was carried out via scanning electron microscopy (SEM). Fig. 2 shows SEM images of samples (1-6). It can be clearly observed that morphology of sample 1 appears to be in the form of nano slices and is entirely different from the morphology of other samples. All other materials show stone like morphology with a distribution of grains having sharp edges, flat surfaces and exhibit a large variation in the size of the grains. This difference might have arisen due to the fact that only sample 1 has single phased monoclinic structure and rest of the materials have mixed phase.

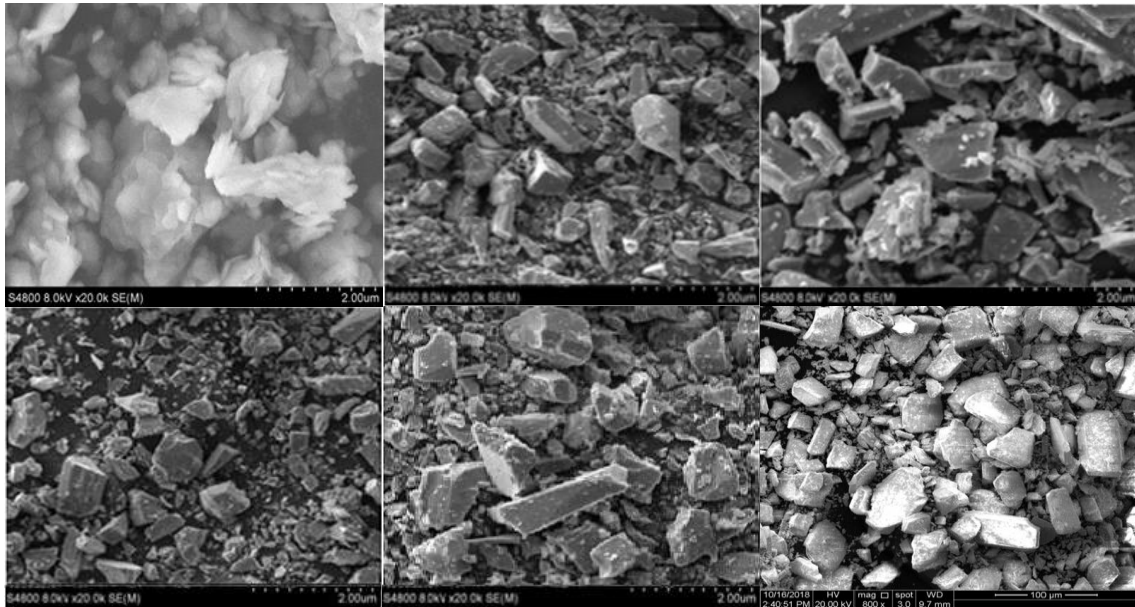


Fig. 2. SEM images of samples 1-6.

### 3.3. Temperature dependent electrical characterization

The electrical characterization was carried out for sample 1 only using two point probe method in temperature range from room temperature to 200°C and from voltage range 0 to 10V. Fig. 3 shows the graph between V and I at different temperatures.

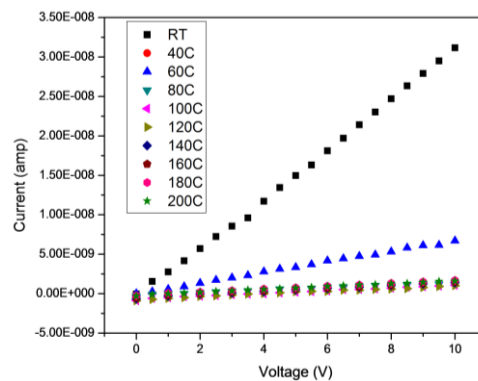


Fig. 3. IV curves for sample 1 at different temperatures.

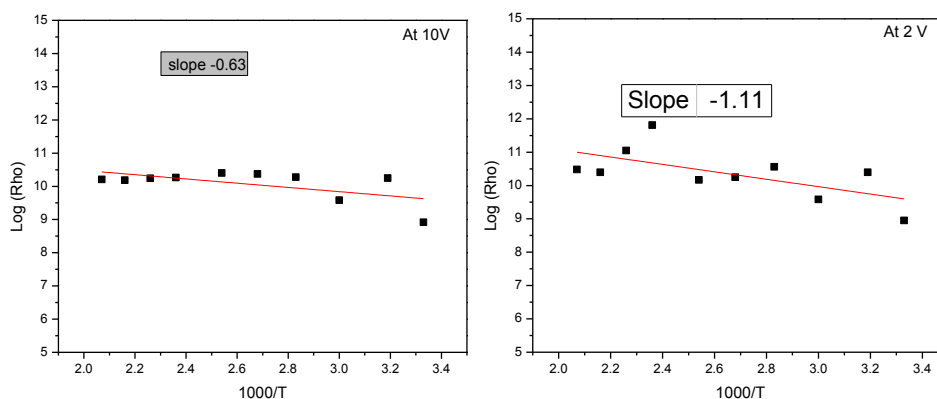


Fig. 4.  $\log(\rho)$  vs.  $1000/T$  graph for sample 1 at 2V and 10V.

The Arrhenius equation was employed to calculate activation energy ( $E_a$ ) at 2V and 10 V.

### 3.4 Electrochemical characterization of CuO modified electrode

Copper oxide modified conductor in buffer solution by examination ratio of 100mV/s can be used to find electrochemical behavior. The electrochemical reactions are inspected in dual system, by Copper oxide improved rods in non-appearance or attendance of hydrogen peroxide. Results showed that cyclic voltammetry (CV) bends of two electrodes display only oxidation peaks. Copper oxide improved electrode owns a great current comeback in presence of  $H_2O_2$  specifying that  $H_2O_2$  presence improves exterior initiation then electron transmission procedures. By using buffer solution, electrochemical reaction of CuO improved electrode was characterized by persistent scan ratio in presence of  $H_2O_2$ . With persistent test degree peak potential don't altered. At constant scan rate peak current linearly varied. The outer surface of CuO modified electrode kinetics corrosion of  $H_2O_2$  was a controlled diffusion process. These results specified that the CuO improved rod showed pointedly best for hydrogen peroxide in positions of reversibility and reckless electron transmission degree.

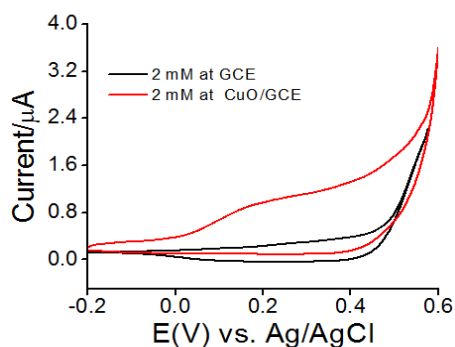
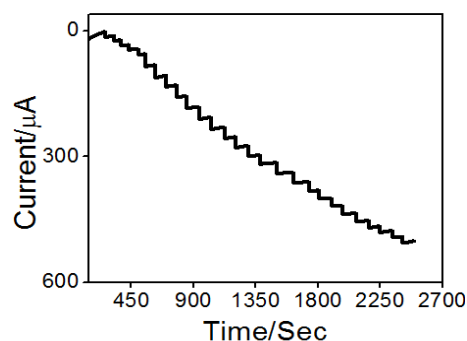


Fig. 5. CuO improved electrode in nonappearance and in occurrence of 2mM and 4mM of hydrogen peroxide on test ratio of 100 mVs.

### 3.5. Sensitivity of Copper Oxide modified electrode

An amperometric measurement was used to determine the sensing capability of the considered electrode. The increasing deliberation of hydrogen peroxide was measured through amperometric measurement. Figure shows that, on a stable voltage CuO improved electrode towards constant doses (2mM) of  $H_2O_2$ . Copper oxide modified deposited glassy carbon electrode shows firm comeback period

approximately 3s, stable value of current, then strong increase in value of current. The extraordinary compassion of CuO improved dropped lustrous carbon rod remains credited, towards exceptional electron allocated hydrophilic exteriors which improved dynamic location diffusion. Aluminum oxide (Al<sub>2</sub>O<sub>3</sub>) deposited polished carbon electrode shows direct regions as of 2–28mM. The exposure limit created on 3 is 1.25mM. CuO deposited polished carbon electrode instrument is better than further non-enzymatic sensors for its short detection boundary or extensive direct variety.



*Fig. 6. Classic amperometric designs of CuO dropped polished carbon electrode by sequential accumulation of 2mM H<sub>2</sub>O<sub>2</sub> by persistent practical potential.*

#### 4. Conclusion

CuO nanomaterials were hydrothermally prepared by employing three different stoichiometric concentrations of reagents. X-ray diffraction (XRD) revealed the presence of single (monoclinic: CuO) and mixed (monoclinic as well as cubic Cu<sub>2</sub>O) phases of copper oxide and cupric oxide respectively. Scanning Electron Microscopy (SEM) images revealed irregular distribution of particles having non-uniform grain shapes of all prepared materials except for the one having pure monoclinic structure. It was further characterized for dc-electrical conductivity followed by electrochemical detection of H<sub>2</sub>O<sub>2</sub>. Results exhibit significant ability of the material towards H<sub>2</sub>O<sub>2</sub> detection.

#### References

- [1] S.M. He, J.S. Li, J. Wang, G.C. Yang, Z.Q. Qiao, *Mat. Lett.* **129**, 5 (2014).
- [2] J.K. Sharma et al., *Journal of Alloys and Compounds* **632**, 321 (2015).
- [3] C. Yang, X. Su, J. Wang, X. Cao, S. Wang, L. Zhang, *Sens. Actuators B* **185**, 159 (2013).
- [4] G. Ren et al., *International Journal of Antimicrobial Agents* **33**, 587 (2009).
- [5] P. Poizat, S. Laruelle, S. Grugeon, L. Dupont, J. M. Tarascon, *Nature* **407**, 496 (2000).
- [6] L. Chen et al., *Journal of Alloys and Compounds* **464**, 532 (2008).
- [7] K. Krishnamoorthy, S. J. Kim, *Mater. Res. Bull.* **48**, 3136 (2013).
- [8] S. Park, S. Kim, S. Park, C. Lee, *Mat. Lett.* **138**, 110 (2014).
- [9] Hafsa Siddiqui, M.S. Qureshi, Fozia. Z. Haque, *Optik* **125**, 4663 (2014).
- [10] I.M.S. Araújo et al., *Carbohydrate Polymers* **179**, 341 (2018).
- [11] Sekhar C. Ray, *Solar Energy Materials & Solar Cells* **68**, 307 (2001).
- [12] B. Toobonsun, P. Singjai, *Journals of alloys compound* **509**, 4132 (2011).
- [13] K. R. Reddy, *Journal of Molecular Structure* **1150**, 553 (2017).

- [14]D. Chirizzi et al., *Talanta***147**, 124 (2016).
- [15] Peng Gao, Dawei Liu, *Sensors and Actuators B* **208**, 346 (2015).
- [16] W. Chen,S.Cai, W. Wen,Y. D. Zhao, *Analyst* **137**, 49 (2012).
- [17]C. Batchelor-McAuley et al., *Sensors and Actuators B: Chemical* **135**(1), 230 (2008).
- [18]Zhang 2012\_Article\_ANovel Non-enzyme Hydrogen Peroxi.pdf.